

## Insight on the electronic state of $\text{Sr}_2\text{IrO}_4$ revealed by cationic substitutions

This article has been downloaded from IOPscience. Please scroll down to see the full text article.

2008 J. Phys.: Condens. Matter 20 295201

(<http://iopscience.iop.org/0953-8984/20/29/295201>)

View [the table of contents for this issue](#), or go to the [journal homepage](#) for more

Download details:

IP Address: 129.252.86.83

The article was downloaded on 29/05/2010 at 13:34

Please note that [terms and conditions apply](#).

# Insight on the electronic state of $\text{Sr}_2\text{IrO}_4$ revealed by cationic substitutions

Y Klein and I Terasaki

Department of Applied Physics, Waseda University, 3-4-1 Ohkubo, Shinjuku-ku, Tokyo 169-8555, Japan

E-mail: [klein@htsc.sci.waseda.ac.jp](mailto:klein@htsc.sci.waseda.ac.jp)

Received 31 March 2008, in final form 5 June 2008

Published 26 June 2008

Online at [stacks.iop.org/JPhysCM/20/295201](http://stacks.iop.org/JPhysCM/20/295201)

## Abstract

We report the electrical resistivity, thermoelectric power and magnetization of  $\text{Sr}_{2-x}\text{La}_x\text{IrO}_4$  ( $x = 0$  and  $0.05$ ) and  $\text{Sr}_2\text{Ir}_{1-y}\text{Rh}_y\text{O}_4$  ( $y = 0.05, 0.1$  and  $0.2$ ) measured below room temperature. In  $\text{Sr}_2\text{IrO}_4$ , electrons (La substitution) or holes (Rh substitution) can be doped, which lead to a strong decrease of the resistivity. In particular, a nearly-metallic state is realized in the case of Rh doping. The thermoelectric power turns out to be metallic-like for  $y = 0.2$ . The presence of a gap in the electronic band structure is robust against these substitutions. From various experimental data, similarities with the 3D charge density wave compound,  $\text{BaBiO}_3$ , are suggested. Nevertheless, rather than a charge density wave, our scenario implies the presence of a spin density wave.

(Some figures in this article are in colour only in the electronic version)

## 1. Introduction

In the past 20 years, 3d transition metal oxides (TMOs) have been extensively studied for their extraordinary properties including the high-temperature superconductivity in cuprates and the colossal magnetoresistance in manganites. Recently, more and more studies are devoted to 4d and 5d TMOs rather than 3d ones. 4d and 5d elements have more extended orbitals, which results in stronger hybridization of neighbouring 4d/5d and O 2p orbitals. As a consequence, we expect weak electron correlation effects and conventional metallic behaviour. Nevertheless, many intriguing properties have been discovered in these compounds and suggest the presence of strongly correlated electrons. In particular, Ru, Rh, Os, Ir and Pt oxides can show features of strongly correlated materials. We can refer to, for example, the ruthenium oxides of the Ruddlesden–Popper (RP) family  $\text{A}_{n+1}\text{Ru}_n\text{O}_{3n+1}$  ( $\text{A} = \text{Ca}$  or  $\text{Sr}$ ), all of which show unusual properties such as superconductivity in  $\text{Sr}_2\text{RuO}_4$  ( $n = 1$ ) with  $T_c = 1.3$  K [1], metal–insulator transition in  $\text{Ca}_3\text{Ru}_2\text{O}_7$  ( $n = 2$ ) with  $T_N = 48$  K [2] and itinerant ferromagnetism in  $\text{SrRuO}_3$  ( $n = \infty$ ) with  $T_c = 163$  K [3]. Among iridium oxides,  $\text{Pr}_2\text{Ir}_2\text{O}_7$  shows spin-liquid behaviour and is described as a frustrated Kondo pyrochlore [4], while  $\text{BaIrO}_3$  shows giant nonlinear conductivity [5].

Here we focus on the transport and magnetic properties of  $\text{Sr}_2\text{IrO}_4$ . This compound adopts the  $I4_1/acd$  space group with a unit cell volume multiplied by four in comparison with  $\text{Sr}_2\text{RuO}_4$  ( $I4/mmm$  space group) [6]. The difference is a rotation of the  $\text{IrO}_6$  octahedra around the  $c$  axis of approximately  $\theta \approx 11^\circ$ . In the ideal structure, the octahedra are alternately turned in a clockwise and anticlockwise direction along the  $c$  axis (figure 1), but neutron diffraction revealed that the sequence of  $\text{IrO}_2$  planes in real samples is subject to disorder [6].  $\text{Sr}_2\text{RhO}_4$  adopts the same structure as  $\text{Sr}_2\text{IrO}_4$ , with a slightly lower angle of rotation,  $\theta \approx 10^\circ$  [7]. Whereas  $\text{Sr}_2\text{RuO}_4$  and  $\text{Sr}_2\text{RhO}_4$  show a metallic resistivity [1, 8],  $\text{Sr}_2\text{IrO}_4$  is a narrow-gap semiconductor with a weak ferromagnetic ground state ( $T_c \approx 240$  K,  $M_s \approx 0.14 \mu_B/\text{Ir}$ ) [9]. For polycrystalline samples, the resistivity is of the order of  $10 \Omega \text{ cm}$  at room temperature and the thermoelectric power shows a broad maximum around 110 K ( $S \approx 300 \mu\text{V K}^{-1}$ ) [10], above which minority carriers are thermally activated. Surprisingly, band calculations and photoemission spectroscopy experiments on  $\text{Sr}_2\text{RuO}_4$  and  $\text{Sr}_2\text{IrO}_4$  give contrasting results concerning the density of states (DOS) at the Fermi level ( $E_F$ ) [11]. On the one hand, the calculated electronic structures of both compounds are similar, with a Fermi level falling in the middle of the  $t_{2g}$  bands. On the other hand, photoemission spectroscopy revealed that  $\text{Sr}_2\text{RuO}_4$  has a finite DOS at  $E_F$ , while  $\text{Sr}_2\text{IrO}_4$  does not. The nature of

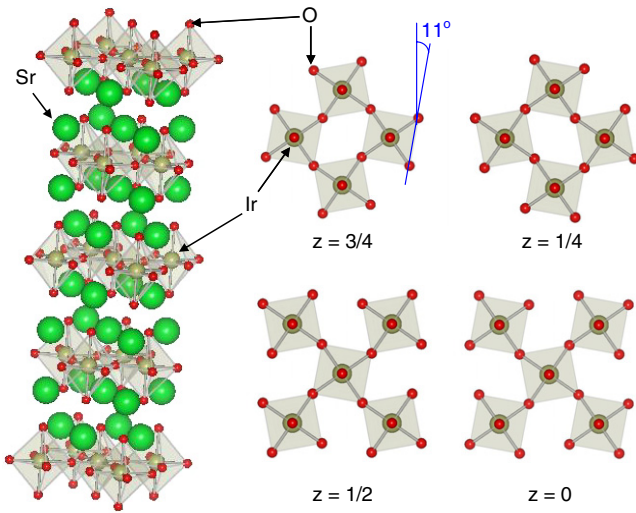


**Figure 1.** Structure of  $\text{Sr}_2\text{IrO}_4$ . Sr, Ir and O elements correspond to large green spheres, medium grey spheres and small red spheres, respectively.

the gap at  $E_F$  has not yet been clarified, but it is found to be responsible for the insulating transport properties of  $\text{Sr}_2\text{IrO}_4$ , which may discriminate 5d TMOs, from two 4d TMOs such as  $\text{Sr}_2\text{RhO}_4$  and  $\text{Sr}_2\text{RuO}_4$ . We expect that the difference in experimental and theoretical results is due to some many-body effect because that kind of phenomenon is not fully considered in band calculations. Although an electronic specific heat was measured to be  $\gamma \approx 2 \text{ mJ K}^{-2} \text{ mol}(\text{Ir})^{-1}$  [10], it does not always mean weak correlation, because the carrier density is reduced by the opening of the gap.

It was reported that  $\text{Ca}^{2+}$  and  $\text{Ba}^{2+}$  can be substituted for  $\text{Sr}^{2+}$  by a small fraction, which does not change the magnetic and transport properties [12]. This may be due to the similar electronic configuration of these three alkaline-earth elements. In the present work, two kinds of cationic substitutions have been tried in order to tune the properties of  $\text{Sr}_2\text{IrO}_4$  and get some insight on its electronic state. Sr has been substituted with La in order to see the response of the material to electron doping. Rh has been inserted on the Ir lattice as a perturbative element of the magnetic environment. Resistivity ( $\rho$ ), thermoelectric power ( $S$ ) and magnetization ( $M$ ) have been measured and analysed. The electrical resistivity itself is insufficient to understand the transport properties because it depends on extrinsic phenomena such as grain-boundary scattering and cannot distinguish n-type from p-type carriers. We need another probe that is less affected by grain boundaries. The thermoelectric power and the Hall coefficient are relevant in the case of polycrystalline samples [13]. Here we show results of thermoelectric power measured below 300 K.

## 2. Experimental details

$\text{Sr}_{2-x}\text{La}_x\text{IrO}_4$  ( $x = 0$  and  $0.05$ ) and  $\text{Sr}_2\text{Ir}_{1-y}\text{Rh}_y\text{O}_4$  ( $y = 0.05, 0.1$  and  $0.2$ ) polycrystalline samples were synthesized from the solid state reaction of  $\text{SrCO}_3$ ,  $\text{IrO}_2$ ,  $\text{La}_2\text{O}_3$  and  $\text{Rh}_2\text{O}_3$  powders. Mixtures were heated in air at  $900^\circ\text{C}$  for 24 h,  $1000^\circ\text{C}$  for

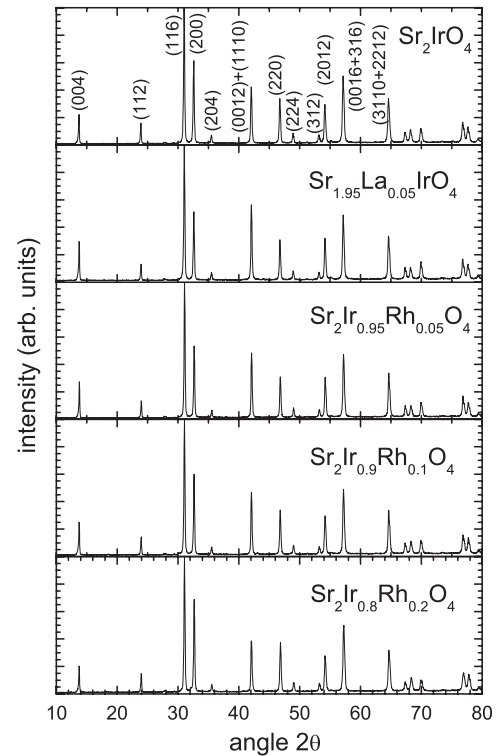


**Figure 2.** X-ray diffraction patterns of the polycrystalline samples  $\text{Sr}_{2-x}\text{La}_x\text{IrO}_4$  ( $x = 0$  and  $0.05$ ) and  $\text{Sr}_2\text{Ir}_{1-y}\text{Rh}_y\text{O}_4$  ( $y = 0.05, 0.1$  and  $0.2$ ). The Cu  $K\alpha$  is used as an x-ray source.

24 h and  $1100^\circ\text{C}$  for 60 h with intermediate grindings. Note that this conventional technique is completely different than the rapid heating and quenching technique used recently to synthesize  $\text{Sr}_{2-x}\text{La}_x\text{IrO}_4$  [14].

The x-ray diffraction was measured using a standard diffractometer with Cu  $K\alpha$  radiation as an x-ray source in the  $\theta$ - $2\theta$  scan mode. The resistivity was measured though a four-terminal method, and the thermoelectric power was measured using a steady-state technique with a typical gradient of  $0.5 \text{ K cm}^{-1}$ . The magnetic properties were studied with a dc SQUID magnetometer (2–400 K, 0–7 T) by recording magnetization as a function of temperature.

### 2.1. Structural analysis

Figure 2 shows the x-ray diffraction patterns of the sintered samples. All the peaks are indexed according to the  $I4_1/acd$  space group. This shows that La and Rh are substituted for Sr and Ir, respectively. For La content exceeding  $x = 0.05$ , we observed a tiny peak corresponding to some unknown impurity. As a consequence, the solubility limit of La to Sr is determined to be  $x = 0.05$ . In figure 3, we plot the evolution of the cell parameters as a function of the La and Rh contents. For the mother compound, the  $a$  and  $c$  axes have been reported many times with different values, ranging from  $5.4921$  to  $5.4994 \text{ \AA}$  for  $a$  and  $25.766$  to  $25.798 \text{ \AA}$  for  $c$  [6, 9, 11, 12, 14, 15]. We calculated the lattice constants to be  $5.4955 \text{ \AA}$  and  $25.783 \text{ \AA}$  for  $a$  and  $c$ , respectively, which are in the range of the reported values. Concerning the effect of

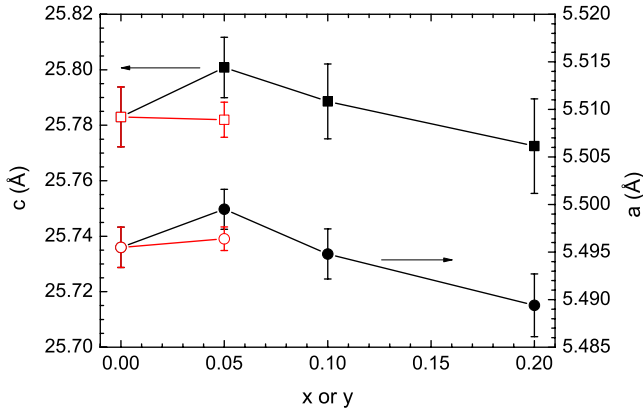


**Figure 3.** Cell parameters,  $a$  axis (circles) and  $c$  axis (squares) of  $\text{Sr}_{2-x}\text{La}_x\text{IrO}_4$  (empty symbols) and  $\text{Sr}_2\text{Ir}_{1-y}\text{Rh}_y\text{O}_4$  (filled symbols).

lanthanum, we observe a slight increase of the  $a$  axis (about  $0.001 \text{ \AA}$ ), and no evolution for the  $c$  axis. On the other hand, Cosio-Castaneda *et al* have reported a more significant increase of  $a$  (about  $0.003 \text{ \AA}$ ) and a decrease of  $c$  (about  $0.021 \text{ \AA}$ ) [14]. The effect of rhodium is more complicated. For 5% Rh content,  $a$  and  $c$  increase and then decrease for higher percentages. As is reported for different perovskites, for example  $\text{AMnO}_{3-\delta}$  manganites ( $A = \text{La, Ca, Sr, etc}$ ), the control of the oxygen stoichiometry is very difficult for non-substituted samples, while it is easier to realize in substituted samples [16]. Considering that oxygen content affects the cell parameters, we think that oxygen non-stoichiometry is a good explanation for the discrepancy noticed before. As a consequence, the  $a$  and  $c$  axis lengths of the  $x = 0$  sample may be different from those for a stoichiometric compound. Higher values would be compatible with the gradual decrease for  $y > 0.05$ .

## 2.2. Properties of the La-doped samples

Figure 4 shows the resistivity and the thermoelectric power of  $\text{Sr}_{2-x}\text{La}_x\text{IrO}_4$  and  $\text{Sr}_2\text{Ir}_{1-y}\text{Rh}_y\text{O}_4$  samples. The La substitution for Sr has a strong effect on the resistivity. The La content of  $x = 0.05$  decreases  $\rho$  by a factor of 10 at 300 K and by a factor of  $10^4$  at 50 K. This suggests that La can provide mobile carriers to  $\text{Sr}_2\text{IrO}_4$ .

Note that the resistivity data of our non-doped and La-doped samples are completely different from those reported by Cosio-Castaneda *et al* [14]. The value of  $\rho$  at room temperature is of the order of  $10 \text{ \Omega cm}$  in both cases but the insulating behaviour is much more pronounced in our sample, as also reported in other references [10, 17, 18]. Furthermore, they reported a smooth and gradual enhancement of the resistivity with increasing La content in contradiction with our strong decrease, even for small La content. This difference can be attributed to different synthesis routes. As mentioned before, they used a fast heating sintering technique and, at the end of the process, quenched their samples. We believe that oxygen contents may be different, which is consistent with different values of lattice parameters. For example,  $c \approx 25.782 \text{ \AA}$  and  $25.746 \text{ \AA}$  for ours and theirs  $\text{Sr}_{1.95}\text{La}_{0.05}\text{IrO}_4$  samples,

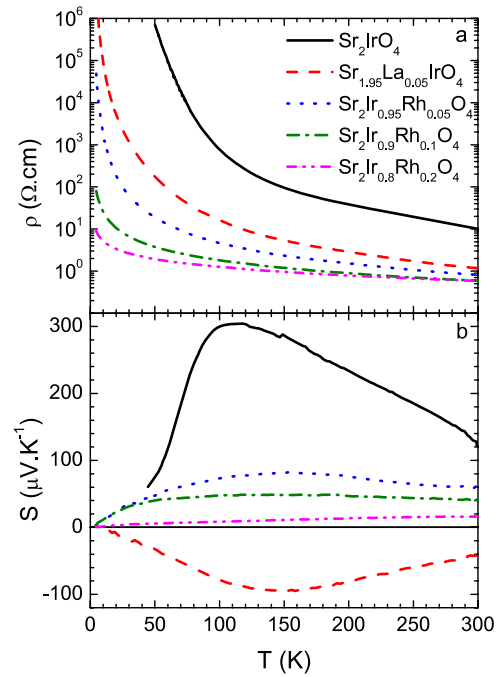


**Figure 4.** Resistivity (a) and thermoelectric power (b) of  $\text{Sr}_{2-x}\text{La}_x\text{IrO}_4$  and  $\text{Sr}_2\text{Ir}_{1-y}\text{Rh}_y\text{O}_4$ .

respectively. In their situation, since the resistivity increases with La content, this cation does not act as a dopant and the increase of the resistivity may be simply related to a structural disorder effect, while in our case, La has a much stronger potential to provide carriers. This hypothesis is shown by the thermoelectric power measurements (see below).

For the non-doped sample,  $S(T)$  rapidly increases from 50 to 110 K, reaches a maximum value of  $305 \mu\text{V K}^{-1}$  and then decreases with increasing temperature to a value of  $120 \mu\text{V K}^{-1}$  at 300 K. The high-temperature decrease indicates that minority carriers, i.e. electrons, are thermally activated through an energy gap of the order of 100 K. For  $x = 0.05$ ,  $S$  changes from large positive values to moderately large negative values. We also measured  $S(T)$  for an  $x = 0.1$  sample, the thermoelectric power of which is identical to that of the  $x = 0.05$  sample, confirming that La cannot supply electrons any more above  $x = 0.05$ . There is also a maximum in the absolute values of  $S \approx -95 \mu\text{V K}^{-1}$  at 150 K, suggesting the activation of minority p-type carriers. The change of the sign of  $S$  for small quantities of La dopant is similar to the situation in semiconducting oxides such as  $\text{LaCoO}_3$  [19]. Below 300 K, both n-type and p-type  $\text{LaCoO}_3$  samples show a large Seebeck coefficient of the order of  $\pm 500 \mu\text{V K}^{-1}$ . But above 350 K,  $S(T)$  curves converge to a small value. High-temperature measurements are now in progress for our samples.

## 2.3. Properties of the Rh-doped samples

The effects of the introduction of Rh on the Ir lattice are quite different. The main effect on the resistivity is to cause much less localized behaviour. For only 5% of Rh substitution,  $\rho$  decreases by a factor of more than 10 at room temperature and by a factor of more than  $10^4$  at 50 K. With

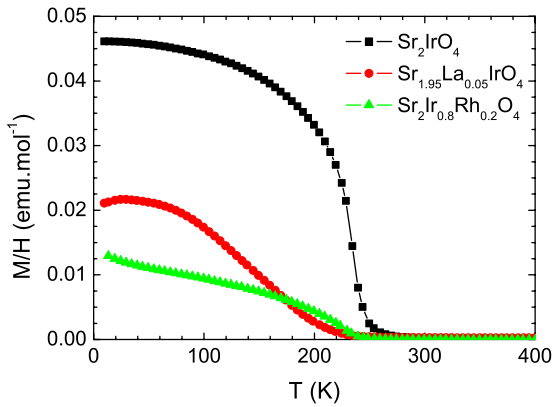


**Figure 5.**  $M/H$  of  $\text{Sr}_2\text{IrO}_4$ ,  $\text{Sr}_{1.95}\text{La}_{0.05}\text{IrO}_4$  and  $\text{Sr}_2\text{Ir}_{0.8}\text{Rh}_{0.2}\text{O}_4$  as a function of temperature measured in a field-cooled process. The applied magnetic field is 0.5 T.

increasing Rh content, the resistivity at room temperature does not decrease so much but the localization is dramatically suppressed by a ratio  $\rho_{x=0}/\rho_{y=0.2}$  of more than  $10^6$  at 50 K. At the same time, the thermoelectric power is strongly decreased and progressively exhibits metallic behaviour with a room temperature value of  $16 \mu\text{V K}^{-1}$  for  $y = 0.2$ . Rhodium can provide  $\text{Ir}^{5+}$  holes if the oxidation state of Rh is  $3+$ . But concomitantly, Rh would act as a strong scattering centre in the  $\text{IrO}_2$  planes, which considerably decreases the carrier mobility. The metallic-like thermoelectric power of the  $y = 0.2$  implies a rather large number of carriers, while the  $x = 0$  sample has fewer carriers activated thermally. As a consequence, to achieve similar values of the resistivity at room temperature, the mobility of the undoped sample is much larger than that of the  $y = 0.2$  samples, which should be examined through the measurement of the Hall constants.

#### 2.4. Magnetization

Figure 5 shows the magnetic susceptibility of  $\text{Sr}_2\text{IrO}_4$ ,  $\text{Sr}_{1.95}\text{La}_{0.05}\text{IrO}_4$  and  $\text{Sr}_2\text{Ir}_{0.8}\text{Rh}_{0.2}\text{O}_4$ . As for the non-doped compound, our data are in accordance with previous results [10, 15]: the ferromagnetic transition occurs below  $T_C \approx 240$  K with an effective moment  $\mu_{\text{eff}} \approx 0.3 \mu_B/\text{Ir}$ . For the substituted samples, the magnitude of the magnetization is decreased. The saturation magnetization is reduced by more than a factor of two for  $x = 0.05$ . This is consistent with recent results published by Cosio-Castaneda *et al* [14]. The magnetization of the Rh-substituted sample monotonically increases below 200 K, which is unconventional in comparison with other ferromagnetic materials. The magnetic interaction between Ir elements is not strongly perturbed by the presence of Rh, even in a quantity as large as 20%.

### 3. Discussion

We will now try to explore possible origins of the energy gap of  $\text{Sr}_2\text{IrO}_4$ . Fukuyama classified insulators among four different categories: band insulators (1), Mott insulators (2), insulators induced by charge ordering (3) and insulators induced by

Anderson localization (4) [20]. Insulating states induced by density waves (3') are special cases of (3).

The transport properties of undoped and doped samples suggest that  $\text{Sr}_2\text{IrO}_4$  is a simple narrow bandgap semiconductor. This is clearly incompatible with the band calculation because a finite DOS at  $E_F$  is predicted. A simple consideration can rule out this possibility: as a consequence of the elongation of the  $\text{IrO}_6$  along the  $c$  axis and the resulting crystal field splitting,  $t_{2g}$  states in  $\text{Sr}_2\text{IrO}_4$  are separated into two degenerated and fully occupied  $d_{yz}$  and  $d_{zx}$  orbitals, and one half-occupied  $d_{xy}$  orbital [21]. Therefore, the system can be considered as a spin-1/2 lattice with one electron per iridium site. According to band theory this system is a metal. On the other hand, the energy gap has been clearly detected at  $E_F$  by photoemission spectroscopy [11, 21].

Now, we consider case (2). Because of the separating  $\text{SrO}$  planes, the electronic interactions between  $\text{IrO}_2$  planes are limited and in-plane interactions dominate the properties. Then, with one electron per lattice, a Mott insulating state is possible if  $U/W \gg 1$ , where  $U$  is the repulsive Coulomb potential and  $W$  is the bandwidth. To our knowledge, values for  $U$  and  $W$  of iridium oxides, including  $\text{Sr}_2\text{IrO}_4$ , have not been reported. Here we compare  $\text{Sr}_2\text{IrO}_4$  with the pyrochlore  $\text{Y}_2\text{Ir}_2\text{O}_7$ , which is regarded as a Mott insulator [22]. A residual  $\gamma$  and a small ferromagnetic moment are common points with  $\text{Sr}_2\text{IrO}_4$ . On the other hand, the transition of the resistivity from non-metallic to metallic behaviour with the substitution of Ca for Y contrasts with the robust insulating state of  $\text{Sr}_2\text{IrO}_4$ .

Due to the quadrupling of the unit cell, one can imagine a splitting of the  $d_{xy}$  band, and therefore a charge order (CO) state, i.e. situation (3), between  $\text{Ir}^{3+}$  and  $\text{Ir}^{5+}$  cations. We can consider two kinds of order, which are an intra-plane order with equivalent planes and an inter-plane order with homogeneous planes of  $\text{Ir}^{3+}$  or  $\text{Ir}^{5+}$ . Regarding the structural, magnetic and transport properties, both situations are unlikely. First, the rotation of the  $\text{IrO}_6$  octahedra around  $c$  keeps the same environment for the iridium cations, i.e.  $\text{IrO}_6$  octahedra are all equivalent if we consider bond lengths and bond angles [6]. From a magnetic point of view, the disproportionation between  $\text{Ir}^{3+}$  ( $t_{2g}^6$ ,  $S = 0$ ) and  $\text{Ir}^{5+}$  ( $t_{2g}^4$ ,  $S = 0$ ) is incompatible with the observation of a ferromagnetic component. Finally, doping should bring some disorder in the  $\text{IrO}_2$  lattice and break the CO state. As a consequence we expect that the resistivity changes to metallic with respect to slight doping [23]. This is not the case in  $\text{Sr}_{1.95}\text{La}_{0.05}\text{IrO}_4$ ,  $\text{Sr}_2\text{Ir}_{1-y}\text{Rh}_y\text{O}_4$  and also in  $\text{Sr}_2\text{Ir}_{1-y}\text{Ru}_y\text{O}_4$ , in which more than 60% of Ru are necessary to induce a metallic state [17].

Anderson localization (4) causes no energy gap [24], which cannot be responsible for the high-temperature insulating state of  $\text{Sr}_2\text{IrO}_4$ .

As an origin of the gap, we propose a charge density wave (CDW) or a spin density wave (SDW) state, case (3'), considering similarities to the perovskite type compound,  $\text{BaBiO}_3$ . In this material, the formal oxidation state of bismuth is  $4+$ , which corresponds to a  $5d^{10}6s^1$  state. As a consequence,  $\text{BaBiO}_3$  is calculated to be a metal with a half-filled  $6s$  conduction band in the band calculation. However, this compound is a semiconductor with a direct optical gap energy  $E_d \approx 1.9$  eV

and a transport activation energy  $E_{ac} \approx 0.24$  eV [25]. The explanation comes from the disproportionation between two inequivalent Bi sites that have a  $\text{Bi}^{(4+\delta)+}$  and a  $\text{Bi}^{(4-\delta)+}$  configuration [26, 27]. This disproportionation can be regarded as a commensurate 3D CDW. We can notice the similarity with  $\text{Sr}_2\text{IrO}_4$  in which the  $d_{xy}$  is half-occupied. Another common feature is that the optical gap is much larger than the activation energy. The gaps of  $\text{Sr}_2\text{IrO}_4$  are evaluated to  $E_d \approx 0.3$  eV [20] and  $E_{ac} \approx 0.056$  eV [18]. The ratio  $E_d/E_{ac}$  is 5.4, which is close to 7.9 for  $\text{BaBiO}_3$ . Finally, according to electrical resistivity, the energy gap of both  $\text{BaBiO}_3$  and  $\text{Sr}_2\text{IrO}_4$  is very robust against doping. In fact,  $\text{Ba}_{1-x}\text{K}_x\text{BiO}_3$  turns out to be metallic for a large amount of K substitution,  $x > 0.35$ , with the particularity of a superconducting state at low temperature [28].  $\text{BaBi}_{1-x}\text{Pb}_x\text{O}_3$  holds the gap for  $x < 0.7$  and suddenly becomes a superconductor for  $x > 0.7$  [29]. A CDW mechanism has been proposed for  $\text{Sr}_2\text{IrO}_4$  on the basis of nonlinear conduction observations [9], but it has been shown later, by more precise measurements, that  $\text{Sr}_2\text{IrO}_4$  exhibits a normal linear resistivity [18]. We should also consider that neutron diffraction patterns do not reveal any superlattice peak due to an ordered state [6]. Furthermore, the susceptibility is Curie–Weiss-like while a CDW is, in general, associated with diamagnetism [30]. For these reasons, we think that an SDW is more probable than a CDW. In  $\text{BaBiO}_3$ , the on-set temperature ( $T_{ON}$ ) for the CDW is given by  $T_{ON} \approx E_d/3.5k_B \approx 6000$  K [25], a temperature higher than the melting point of the material. This model, applied to the eventual SDW in  $\text{Sr}_2\text{IrO}_4$ , gives a lower value  $T_{ON} \approx 1000$  K, but still too high to observe any transition on the magnetic or transport curves. In that case, the pinning force of the CDW or SDW is too strong to observe nonlinear conduction or magnetoresistance due to a ‘sliding’ of the density wave. In fact, a 12 T magnetic field does not induce any magnetoresistance in  $\text{Sr}_2\text{IrO}_4$  single crystals [9]. In order to detect the existence of an SDW order, we think that nuclear magnetic resonance and/or muon spin relaxation will be effective.

#### 4. Conclusion

In conclusion, we have synthesized n-type and p-type  $\text{Sr}_2\text{IrO}_4$  by using cationic substitutions. The resistivity is strongly decreased for small contents of Rh or La, but keeps a semiconducting dependence. With the Rh substitution for Ir, the localization at low temperature is strongly suppressed and the thermoelectric power progressively evolved to a metallic behaviour. At first glance,  $\text{Sr}_2\text{IrO}_4$  seems to be a normal band insulator, which is incompatible with the electronic configuration of the half-filled  $d_{xy}$  band. Therefore, we believe that  $\text{Sr}_2\text{IrO}_4$  is not a band insulator and that the gap comes from many-body effects. As neutron diffraction did not reveal any superlattice structure, charge order and charge density wave are unlikely to occur. Although the possibility of a Mott insulator cannot be discarded, we propose that a two-dimensional spin density wave is an alternative origin for the gap. More experiments are needed to clarify the electronic state of  $\text{Sr}_2\text{IrO}_4$ .

#### Acknowledgments

We thank S Shibasaki for technical support. This work was supported by the Academic Frontier Project from MEXT. YK

is a research fellow of the Japanese Society for the Promotion of Science.

#### References

- [1] Maeno Y, Hashimoto H, Yoshida K, Nashizaki S, Fujita T, Bednorz J G and Lichtenberg F 1994 *Nature* **372** 532
- [2] Cao G, McCall S, Crow J E and Guertin R P 1997 *Phys. Rev. Lett.* **97** 1751
- [3] Kobayashi H, Nagata M, Kanno R and Kawamoto Y 1994 *Mater. Res. Bull.* **29** 1271
- [4] Nakatsuji S, Machida Y, Maeno Y, Tayama T, Sakakibara T, Van Duijn J, Balicas L, Millican J N, Macaluso R T and Chan J Y 2006 *Phys. Rev. Lett.* **96** 087204
- [5] Nakano T and Terasaki I 2006 *Phys. Rev. B* **73** 195106
- [6] Huang Q, Soubeyrou J L, Chmaissem O, Natali Sora I, Santoro A, Cava R J, Krajewski J J and Peck W F Jr 1994 *J. Solid State Chem.* **112** 355
- [7] Subramanian M A, Crawford M K, Harlow R L, Ami T, Fernandez-Baca J A, Wang Z R and Johnston D C 1994 *Physica C* **235** 743
- [8] Perry R S, Baumberger F, Balicas L, Kikugawa N, Ingle N J C, Rost A, Mercure J F, Maeno Y, Shen Z X and Mackenzie A P 2006 *New J. Phys.* **8** 175
- [9] Cao G, Bolivar J, McCall S, Crow J E and Guertin R P 1998 *Phys. Rev. B* **57** R11039
- [10] Kini N S, Strydom A M, Jeevan H S, Jeevan C, Geibel C and Ramakrishnan S 2006 *J. Phys.: Condens. Matter* **18** 8205
- [11] Rama Rao M V, Sathe V G, Sornadurai D, Panigrahi B and Shripathi T 2000 *J. Phys. Chem. Solids* **61** 1989
- [12] Shimura T, Inaguma Y, Nakamura T and Itoh M 1995 *Phys. Rev. B* **52** 9143
- [13] Carrington A and Cooper J R 1994 *Physica C* **219** 119
- [14] Cosio-Castaneda C, Tavizon G, Baeza A, De La Mora P and Escudero R 2007 *J. Phys.: Condens. Matter* **19** 446210
- [15] Crawford M K, Subramanian M A, Harlow R L, Fernandez-Baca J A, Wang Z R and Johnston D C 1994 *Phys. Rev. B* **49** 9198
- [16] Rormark L, Wiik K, Stolen S and Grande T 2002 *J. Mater. Chem.* **12** 1058
- [17] Cava R J, Batlogg B, Kiyono K and Takagi H 1994 *Phys. Rev. B* **49** 11890
- [18] Fisher R, Genossar J, Knizhnik A, Patlagan L and Reisner G M 2007 *J. Appl. Phys.* **101** 123703
- [19] Hébert S, Flahaut D, Martin C, Lemonnier S, Noudem J, Goupil C, Maignan A and Hejtmanek J 2007 *Prog. Solid State Chem.* **35** 457
- [20] Fukuyama H 2005 *Japan Nanonet Bulletin* <http://www.nanonet.go.jp/english/mailmag/2005/038a.html>
- [21] Moon S J, Kim M W, Lee Y S, Kim J-Y, Park J-H, Kim B J, Oh S-J, Nakatsuji S, Maeno Y, Nagai I, Ikeda S I, Cao G and Noh T W 2006 *Phys. Rev. B* **74** 113104
- [22] Fukazawa H and Maeno Y 2002 *J. Phys. Soc. Japan* **71** 2578
- [23] Imada M, Fujimori A and Tokura Y 1998 *Rev. Mod. Phys.* **70** 1039
- [24] Anderson P W 1958 *Phys. Rev.* **109** 1492
- [25] Uchida S, Kitazawa K and Tanaka S 1987 *Phase Transit.* **8** 95
- [26] Bischofs I B, Kostur V N and Allen P B 2002 *Phys. Rev. B* **65** 115112
- [27] Allen P B and Bischofs I B 2002 *Phys. Rev. B* **65** 115113
- [28] Ahmad J, Yamanaka H and Uwe H 2007 *J. Phys.: Condens. Matter* **19** 266223
- [29] Cava R J, Batlogg B, Krajewski J J, Farrow R, Rupp L W Jr, White A E, Short K, Peck W F and Kometani T 1988 *Nature* **332** 28
- [30] Sleight A W, Gilson J L and Bierstedt P E 1975 *Solid State Commun.* **17** 27
- [31] Grüner G 1994 *Density Waves in Solids* (Reading, MA: Addison-Wesley)